ACS OMEGA

Article

Cite This: ACS Omega 2019, 4, 9531−9541

http://pubs.acs.org/journal/acsodf

Azadirachtin-A from *Azadirachta indica* Impacts Multiple Biological Targets in Cotton Bollworm *Helicoverpa armigera*

Vishal V. Dawkar,[*,†,⊥] Sagar H. Barage,[§,∥] Ranjit S. Barbole,[†] Amol Fatangare,[⊥] Susana Grimalt,[⊥] Saikat Haldar,[‡] David G. Heckel,[#] Vidya S. Gupta,[†] Hirekodathakallu V. Thulasiram,[‡] Aleš Svatoš,[⊥] and Ashok P. Giri[†]

[†]Plant Molecular Biology Unit, Division of Biochemical Sciences and [‡]Division of Organic Chemistry, CSIR-National Chemical Laboratory, Dr. Homi Bhabha Road, Pune 411008, Maharashtra, India

[§]Bioinformatics Centre, Savitribai Phule Pune University, Ganeshkhind Road, Pune 411007, Maharashtra, India

[∥]Amity Institute of Biotechnology (AIB), Amity University, Mumbai−Pune Expressway, Bhatan, Post-Somathne, Panvel, Mumbai 410206, Maharashtra, India

[⊥]Research Group, Mass Spectrometry/Proteomics and [#]Department of Entomology, Max Planck Institute for Chemical Ecology, 07745 Jena, Germany

Supporting Information

ABSTRACT: Azadirachtin-A (AzaA) from the Indian neem tree (*Azadirachta indica*) has insecticidal properties; however, its molecular mechanism remains elusive. The "targeted and nontargeted proteomic profiling", metabolomics, matrix-assisted laser desorption/ionization time of flight (MALDI-TOF) imaging, gene expression, and in silico analysis provided clues about its action on *Helicoverpa armigera*. Fourth instar *H. armigera* larvae fed on AzaA-based diet (AzaD) suffered from significant mortality, growth retardation, reduced larval mass, complications in molting, and prolonged development. Furthermore, death of AzaD-fed larvae was observed with various phenotypes like bursting, blackening, and half-molting. Liquid chromatography−mass spectrometry (LC−MS) data showed limited catabolic processing of ingested AzaA and dramatic alternations of primary metabolism in *H. armigera*. MALDI-TOF imaging indicated the presence of AzaA in midgut of *H. armigera*. In the gut, out of 79 proteins identified, 34 were upregulated, which were related to digestion, immunity, energy production, and apoptosis mechanism. On the other hand, 45 proteins were downregulated, including those from carbohydrate metabolism, lipid metabolism, and energy transfer. In the hemolymph, 21 upregulated proteins were reported to be involved in immunity, RNA processing, and mRNA-directed protein synthesis, while 7 downregulated proteins were implicated in energy transfer, hydrolysis, lipid metabolism, defense mechanisms, and amino acid storage-related functions. Subsequently, six target proteins were identified using labeled AzaA that interacted with whole insect proteins. In silico analysis suggests that AzaA could be efficiently accommodated in the hydrophobic pocket of juvenile hormone esterase and showed strong interaction with active site residues, indicating plausible targets of AzaA in *H. armigera*. Quantitative polymerase chain reaction analysis suggested differential gene expression patterns and partly corroborated the proteomic results. Overall, data suggest that AzaA generally targets more than one protein in *H. armigera* and hence could be a potent biopesticide.

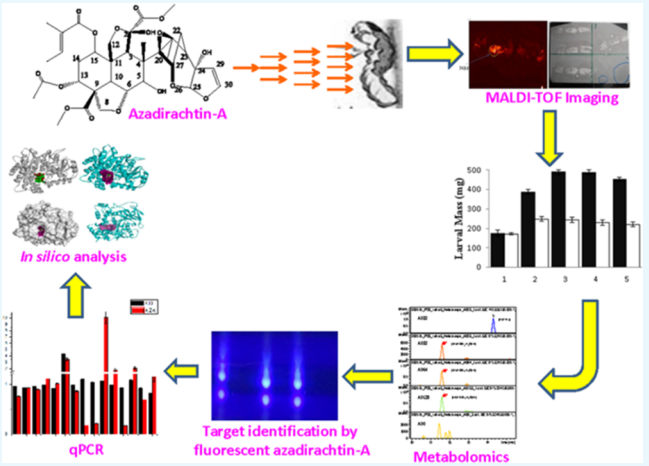

INTRODUCTION

The neem tree (*Azadirachta indica*) has long been recognized for its unique properties, both against insects and in improving human health.[1,2] Azadirachtin-A (AzaA) is a well-known tetranortriterpenoid limonoid phytochemical and natural pesticide molecule.[3−5] It is present in seed, leaves, and other parts of the neem tree. It is known as a feeding deterrent and a strong growth disruptant for many arthropods. Interestingly, it is remarkably nontoxic to vertebrates. AzaA has a very complex structure; hence, it took nearly 17 years to elucidate its full structure. Unlike many other plant compounds, AzaA alone is a strong antifeedant and thus exploited commercially. There is an implicit assumption that AzaA strongly influences insect

Received: December 12, 2018
Accepted: March 11, 2019
Published: May 31, 2019

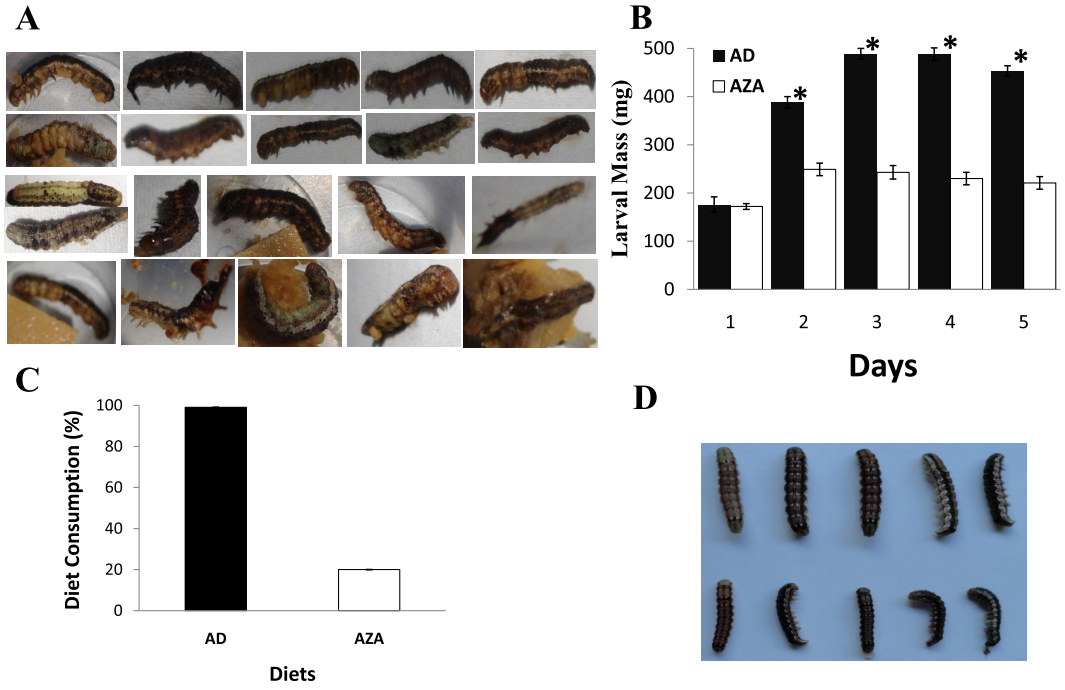

Figure 1. Growth performance and phenotypic observations of *H. armigera* reared on AzaD and artificial diet (AD) diets. (A) Phenotypic observations of AzaD-fed *H. armigera* showing bursting of whole insect, seizing of molting, and many more phenotypes. (B) Larval mass fed on AzaD (hollow bars) and AD diet (black bars). The graph shows average mass from each set of 15 larvae. Larvae were critically weighed after every 24 h. (C) Diet consumption data of *H. armigera* reared on AzaD and AD diets. Larvae fed on AD finished all diet (~99.99%) in 4 days (black bar), whereas insects fed on AzaD could consume only ~20% of the total diet (hollow bars). (D) Photograph of larvae grown on an AzaD showing stunted growth (bottom row) and AD diet showing normal growth (top row).

hormones through interference with the neuroendocrine system.

Many attempts have been made to understand the molecular action of AzaA in various insect species.[6−13] AzaA's structure is multifaceted, complicating an understanding of its chemistry.[1,14−16] It interferes with the molting of insects and has growth regulatory and sterilant effects.[8] Its action as an antagonist of the molting hormone and therefore its ability to cause alterations in the development of insects, as well as its effects on their reproductive ability, have been widely documented, especially in Lepidoptera.[8] Moreover, in most of the cases, it also produces a disruption of their feeding habits.[17]

Helicoverpa armigera (Lepidoptera: Noctuidae; Hübner) is a devastating pest of many important crop plants throughout the world and thus responsible for heavy economic losses.[18] This pest feeds actively on various plants for development and progression into the reproductive adult phase. However, current strategies for the control of *H. armigera* have relied heavily on conventional chemical control, resulting in the development of resistance in *H. armigera* to almost all of the insecticides (www.pesticideresistance.org/; www.iraconline.org/).[19,20] Considerable research has demonstrated the potential of insects to adapt to diverse phytochemicals and toxins.[21−23]

Most insecticides have a single highly conserved protein target, thereby not only harming beneficial insects but also facilitating resistance evolution in pests. Hence, a pesticide with multiple targets without harmful ecological effects is needed. This motivated us to understand the mechanism and toxicity of AzaA in *H. armigera*. Feeding experiments using AzaA in *H. armigera* confirmed that it is a strong antifeedant and growth disrupter and showed insecticidal potency. Here, we report the distribution of AzaA in *H. armigera*, as determined by matrix-assisted laser desorption/ionization time of flight (MALDI-TOF) imaging. The presence of AzaA in the insect was confirmed independently. The comparative molecular approach revealed differences in gut and hemolymph of *H. armigera* reared on artificial diet with or without AzaA. Striking alterations of primary metabolism were observed upon ingestion of AzaA by the insects. Pull-down assays with labeled AzaA identified several proteins like apolipophorin III, mannose 6 phosphate isomerase, fatty acid binding protein (FABP), diguanylate cyclase, juvenile hormone esterase (JHE), and arylphorin, indicating there are multiple targets of AzaA in *H. armigera*.

RESULTS

Antibiosis of AzaA to *H. armigera* Larvae. To evaluate the effect of AzaA, our observations of larvae fed on AzaA-based diet (AzaD) showed a variety of diverse phenotypes, including bursting of the whole insect, molting arrest, and many others (Figure 1A). As expected, food consumption and larval mass were dramatically reduced (Figure 1B,C). The larvae fed on AzaD showed stunted growth (Figure 1D). These results confirmed that AzaA is a potent insect antifeedant with growth-disrupting properties as reported earlier. This phenotypic diversity suggested that AzaA could have several targets for its toxic mode of action.

MALDI-TOF Imaging Detected AzaA in the Midgut of *H. armigera*. We investigated the localization of AzaA in the midgut of *H. armigera* by axial MALDI-TOF imaging of insect cross sections with a 2,5-dihydroxybenzoic acid (DHB) matrix that provided a uniform deposition of a matrix ion (Figure

DOI: 10.1021/acsomega.8b03479
ACS Omega 2019, 4, 9531−9541

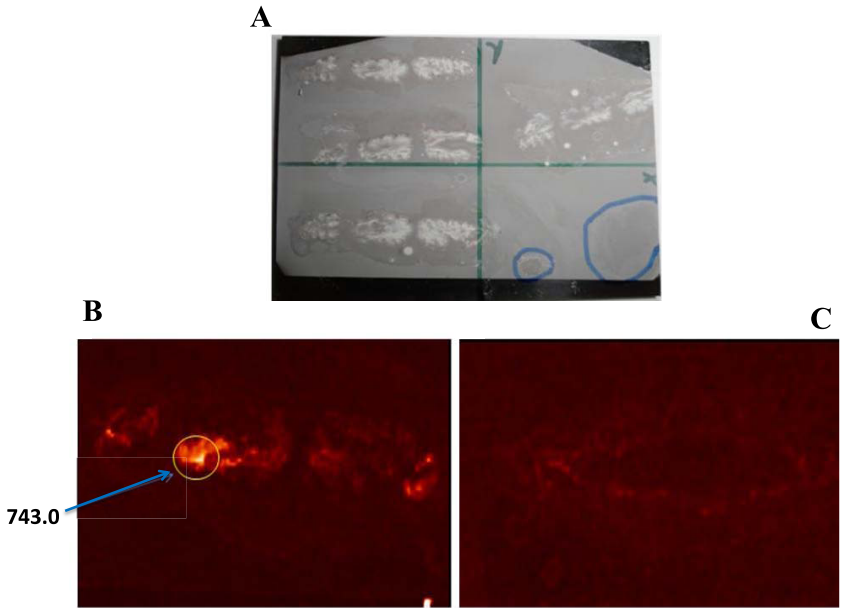

Figure 2. Mass spectrometric imaging (LDI-TOF/MS) of *H. armigera*. (A) Photograph of the insect used for LDI-TOF/MS imaging mounted on a MALDI target plate. (B) MALDI imaging of *H. armigera* showing AzaA in the midgut of AzaD-fed insect (white area, m/z 743 ± 0.5 $[M + Na]^+$). (C) AD-fed *H. armigera* did not show signal for AzaA after LDI-TOF/MS imaging.

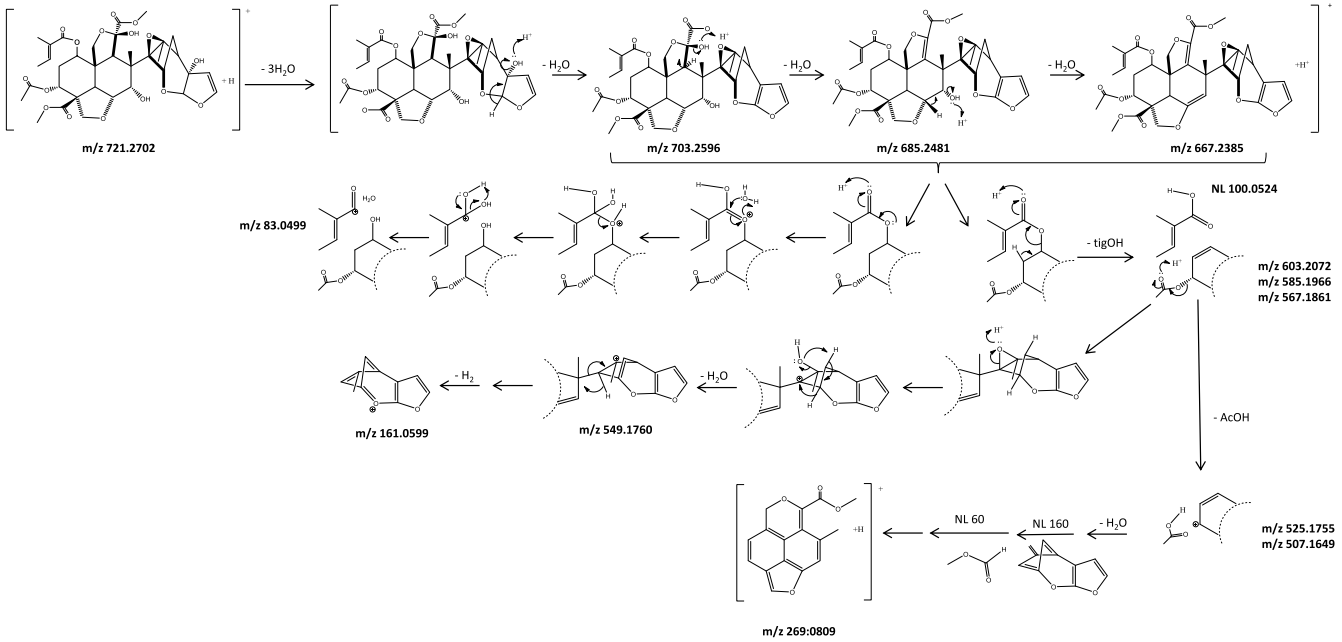

Figure 3. Proposed pathway for AzaA in *H. armigera*. Proposed pathway for AzaA designed on the basis of degradation products found during LC–MS analysis extracted from AzaA-fed larvae.

2A). The experimental protocol used was sensitive, yielding mass spectra with clear signals for the $[M + Na]^+$ ion of AzaA from very low amounts (64 ppm in the diet). The chemical identity of the compound was confirmed by mass spectrometry analysis. In the MS spectrum of AzaA, the molecular peak at m/z 743.25 corresponds to the $[M + Na]^+$ adduct ion. MALDI-TOF spectra were collected from the whole insect in both *X* and *Y* directions. Conversion of the ion chromatogram into ion intensity images showed a distribution of AzaA within the midgut of larvae (Figure 2B). Statistical evaluation indicated that AzaA was present only in the midgut of the insect. As expected, the larvae reared on diet lacking AzaA (AD) did not show any signal for AzaA (Figure 2C).

Metabolomic Analysis Indicates Minimal AzaA Catabolism while Strongly Affecting Primary Metabolism in *H. armigera*. First, we have annotated the most important mass fragments by proposing the fragmentation pathway of the AzaA (Figure 3, Suppl. Figures 2 and 3). This information will be of interest for future mass spectrometric studies where AzaA precursor analyte and its transformation products/metabolites can be correlated. Further in the metabolomics analysis, we focused on the potential biotransformation and/or catabolism of AzaA. Based on common

DOI: 10.1021/acsomega.8b03479
ACS Omega 2019, 4, 9531−9541

Table 1. Proposed Degradation Transformation for AzaA and the Peaks Found in LC−MS Positive Mode Full Mass Scan Spectra

proposed transformation	description	chemical formula	mass change (Da)	TP exact mass (Da)	m/z deviation $[M + H]^+$ (mDa)	Rt (min)
double-bond hydration position 29−30	$+H_2O$	$C_{35}H_{46}O_{17}$	+18.01056	738.2735		
double-bond hydration position 48−49	$+H_2O$	$C_{35}H_{46}O_{17}$	+18.01056	738.2735		
hydrolysis methyl esther position 2	$-CH_2$	$C_{34}H_{42}O_{16}$	−14.0157	706.2472	2.8	13.50 (+)
hydrolysis methyl esther position 9	$-CH_2$	$C_{34}H_{42}O_{16}$	−14.0157	706.2472	2.8	13.50
dehydration to double-bond position 24−25	$-H_2O$	$C_{35}H_{42}O_{15}$	−18.0105	702.2523	0.3	15.04
dehydration to double-bond position 5−6	$-H_2O$	$C_{35}H_{42}O_{15}$	−18.0105	702.2523	0.3	15.04
dehydration to double-bond position 2−3	$-H_2O$	$C_{35}H_{42}O_{15}$	−18.0105	702.2523	0.3	15.04
desacetylation position 13	$-C_2H_2O$	$C_{33}H_{42}O_{15}$	−42.0106	678.2523		
hydrolysis methyl esther 2	$-C_2H_2O$	$C_{33}H_{42}O_{15}$	−42.0106	678.2523		
hydrolysis methyl esther 9	$-C_2H_2O$	$C_{33}H_{42}O_{15}$	−42.0106	678.2523		
hydrolysis tiglic acid position 15	$-C_5H_6O$	$C_{30}H_{38}O_{15}$	−82.0418	638.2211		11.8 (+)
hydrolysis + double-bond hydration	$-CH_2 + H_2O$	$C_{34}H_{44}O_{17}$	3.9949	724.2578		11.0
hydrolysis + dehydratation to double bond	$-CH_2 - H_2O$	$C_{34}H_{40}O_{15}$	−32.0262	688.2367	0.2	13.71
2 × hydrolysis	$2 \times (-CH_2)$	$C_{33}H_{40}O_{16}$	−28.0313	692.2316	3.0	14.14
2 × hydrolysis + dehydratation to double bond	$2 \times (-CH_2) - H_2O$	$C_{33}H_{38}O_{15}$	−46.0419	674.2211	0.1	11.60

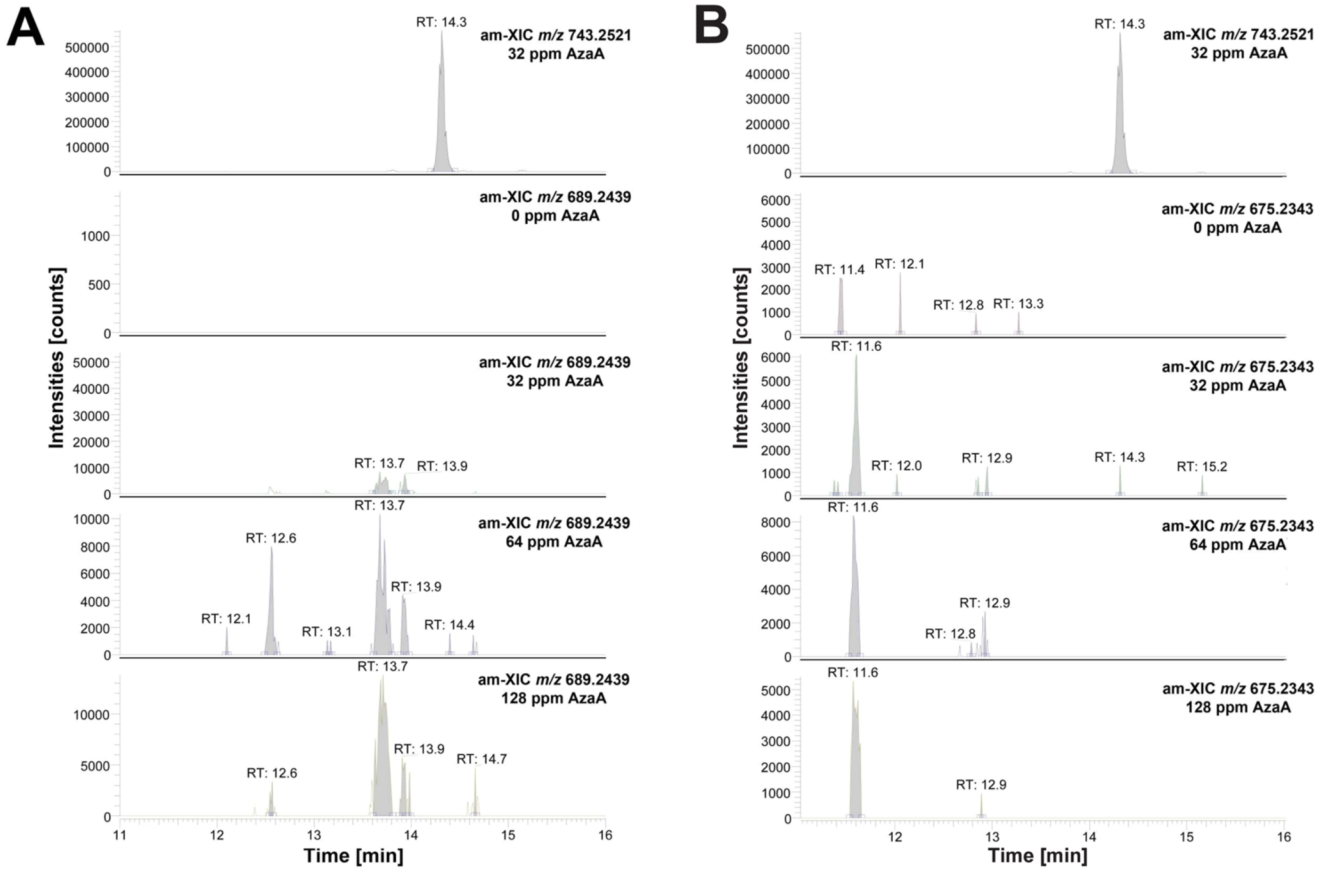

Figure 4. LC-electrospray ionization (ESI)(+)-Q-Exactive MS accurate mass-extracted ion chromatogram (am-XIC) for AzaA metabolites and proposed fragmentation pathway for the $[M + Na]^+$ of azadirachtin-A. (A) LC-ESI(+)-Q-Exactive MS am-XIC chromatogram for m/z 743.2521 on AzaA 32 ppm; and m/z 689.2439, $[(AZA\text{-}CH_2\text{-}H_2O) + H]^+$, on AzaA 32 ppm, AzaA 64 ppm, AzaA 128 ppm, and AzaA 0 ppm. (B) LC-ESI(+)-Orbitrap MS am-XIC chromatogram for m/z 743.2521 on AzaA 32 ppm; and m/z 675.2343, $[(AZA\text{-}2CH_2\text{-}H_2O) + H]^+$, on AzaA 32 ppm, AzaA 64 ppm, AzaA 128 ppm, and AzaA 0 ppm.

detoxification pathways, biotransformation metabolites were proposed (Suppl. Table 5). Out of 35 proposed biotransformation products from AzaA, 9 have been found in the liquid chromatography−mass spectrometry (LC−MS) and mentioned in Suppl. Table 5. However, to confirm the presence of these metabolites, the study of the product ion scan of those compounds will be necessary. Most probable degradation products of AzaA are shown in Table 1. An interesting consideration to consider is the combination of the biotransformations. Figures 4A,B and 5 show accurate mass-extracted ion chromatogram (am-XIC) traces in LC−MS for two predicted most abundant potential metabolites from AzaA, $[(AZA\text{-}CH_2\text{-}H_2O) + H]^+$ and $[(AZA\text{-}2CH_2\text{-}H_2O) + H]^+$. Both results are from saponification of either one or two methylester

DOI: 10.1021/acsomega.8b03479
ACS Omega 2019, 4, 9531−9541

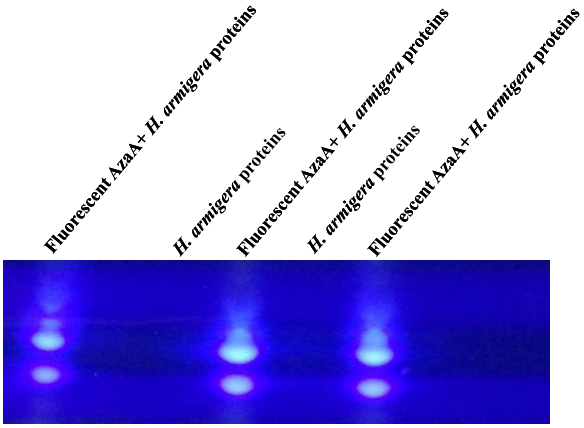

Figure 5. Native polyacrylamide gel electrophoresis (PAGE) protein profile of whole *H. armigera* larval proteins with labeled AzaA. Native PAGE protein profile of AD-fed larval proteins in the presence of fluorescently labeled AzaA. 7-Nitrobenzo-2-oxa-1,3-diazole (NBD)-labeled AzaA upon incubation with AD-fed whole larval proteins showed fluorescence; conversely, only AD-fed larval proteins did not show any signal.

groups of AzaA (Table 1). The intensities of additional AzaA metabolite's peaks were low (below 1%) in comparison to AzaA peak, which confirms that AzaA is not transformed into other metabolites to a significant degree. Intact AzaA was detected in *H. armigera* larvae fed with 32−128 ppm concentration range of AzaA as the corresponding $[M + H]^+$ and $[M + Na]^+$ ions. The total intensity of the ions is shown in Suppl. Figure 4. At the lowest concentration (32 ppm), the signal dramatically increased from that in normal AD-fed larvae. However, the amounts of AzaA in larvae fed on higher AzaD did not increase proportionately. It may be explained by the deterrent effect of AzaA as larvae have fed less on diet with increasing AzaA levels (Figure 1C).

In the metabolomics analysis, we further investigated the AzaA effect on the general metabolism/catabolism of *H. armigera*. About 30 primary metabolites like amino acids (AAs), fatty acids, intermediates in glycolysis and the citrate cycle, UDPs, and sugars were evaluated in relation to AzaA feeding group, as shown in Suppl. Data 1 (see also Suppl. Data 2−4). Three basic trends were observed: (i) no change, (ii) metabolite downregulation, and (iii) metabolite upregulation after feeding on AzaD. Diverse patterns were observed for amino acids (AAs). While lysine, arginine, and glutamate increased, histidine, serine, glutamine, and proline did not change. Many of the AAs from the list, such as asparagine, aspartate, leucine, phenylalanine, threonine, tyrosine, etc., were dramatically down at 128 ppm AzaA. Among the down-regulated AAs, asparagine, phenylalanine, and threonine showed decreased levels even at 32 ppm dose. In contrast, cysteine, methionine, and tryptophan increased at 32 ppm dose that later decreased. All studied fatty acids and other neutral lipids gradually decreased (data not shown). The citrate cycle was also affected by AzaA treatment. Citrate and succinate initially increased to 32 ppm and further decreased with increase in AzaA level. Overall, strong primary metabolite alterations were observed even at the lowest AzaA amount (32 ppm).

Proteomic Patterns in *H. armigera* upon Exposure to the AzaA. A comparative proteomic approach was used to investigate the protein differences in gut and hemolymph of *H. armigera* reared on AD and AzaD. In this study, 107 differentially expressed proteins from gut and hemolymph of AzaD-fed *H. armigera* were identified by nano-LC−MS^E. Database searches combined with gene ontology (GO) analysis were used to infer the functions of proteins identified. Among the 79 proteins identified in the gut, 34 proteins related to digestion, immunity, energy production, and apoptosis mechanism were upregulated, while 45 proteins involved in carbohydrate and lipid metabolism and energy transfer were downregulated (Suppl. Table 3). In hemolymph, among 28 proteins, the 21 upregulated proteins were involved in immunity, RNA processing, and mRNA-directed protein synthesis, while the 7 downregulated proteins were implicated in energy transfer, hydrolysis, lipid metabolism, defense mechanisms, and amino acid storage-related functions (Suppl. Table 4). Overall, from gut and hemolymph, 55 proteins were upregulated, while 52 proteins were down-regulated in AzaD-fed *H. armigera*.

Targeted Proteomic Analysis Identifies Several Targets of AzaA in *H. armigera*. By using fluorescently labeled AzaA (NBD-based), targeted proteomic analysis was performed with PAGE. A native PAGE protein profile of *H. armigera* after incubation with labeled AzaA is shown in Figure 4. Fluorescent protein bands were cut and subsequently identified using mass spectrometry. Protein identification by search with the NCBI insects database identified six proteins, viz., apolipophorin III, mannose 6 phosphate isomerase, fatty acid binding protein, diguanylate cyclase, juvenile hormone esterase (JHE), and arylphorin.

Gene Expression Analysis of *H. armigera* upon AzaA Exposure. From the differentially regulated proteins, we selected 15 candidate genes for expression analysis. Transcripts of six of these genes (glyceraldehyde 3 phosphate dehydrogenase—GAPDH, aminopeptidase, trypsin isoforms 1 and 2, acyl CoA binding protein, and a heat shock protein) were upregulated in AzaD-fed *H. armigera* larvae and transcripts of cathepsin, fatty acid binding protein, arginine kinase, arylphorin, chymotrypsin, JHE, trypsin isoform 3, and carboxypeptidase were downregulated (Figure 6). However, superoxide dismutase (SOD) (Cu/Zn) remained constant in both the AD- and AzaD-fed *H. armigera*. Trypsin isoforms exhibited complexity in expression profiles. Trypsin isoforms 1 and 2 were found to be most abundant in gut tissue of AzaD-fed insects, and trypsin 1 showed nearly 10 times higher expression than the rest of the isoforms, while in gut tissue of AzaD-fed insects, levels of trypsin isoform 3 were decreased. AzaD-fed larvae showed ∼8× downregulation of the chymotrypsin gene expression compared to AD-fed larvae, while acyl CoA binding protein and heat shock protein were significantly upregulated in AzaD-fed *H. armigera*. Except for superoxide dismutase (Cu/Zn) and glyceraldehyde 3 phosphate dehydrogenase, the other genes were significantly differentially expressed in either AD- or AzaD-fed *H. armigera*.

Molecular Interaction of AzaA with JHE from *H. armigera*. The proteomic and gene expression analysis data upon AzaD exposure suggested that JHE, a key enzyme involved in insect development and metabolism, could be one of the probable targets of AzaA. We therefore explored the interaction between JHE and AzaA with the help of molecular docking using AutoDock 4.2.[24] To validate the docking protocol, we extracted 3-octylthio-1,1,1-trifluoropropan-2-one (OTFP) from the co-crystal structure of JHE (PDB ID: 2FJ0) and redocked OTFP with JHE.[25] The docked conformation of

DOI: 10.1021/acsomega.8b03479
ACS Omega 2019, 4, 9531−9541

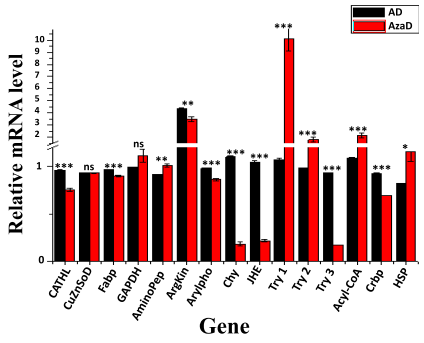

Figure 6. Quantitative real-time reverse transcription-polymerase chain reaction (RT-PCR) analysis. Quantitative real-time RT-PCR analysis of mRNA transcript abundance of selected cathepsin, superoxide dismutase Cu Zn, fatty acid binding protein, glyceraldehyde 3 phosphate dehydrogenase, aminopeptidase, arginine kinase, arylphorin, chymotrypsin, juvenile hormone esterase, trypsin, acyl CoA binding protein, carboxypeptidase, and heat shock protein genes with RNA extracted from gut tissue of *H. armigera* larvae reared on AD and AzaD, respectively. The *Y* axis represents the relative gene expression ratio calculated using the standard relative plot method. The error bars represent standard deviation in three biological replicates. *, **, and *** indicate that values are significantly different from each other at $p < 0.01$, $p < 0.001$, and $p < 0.0001$, respectively.

OTFP shows an root-mean-square deviation (RMSD) of 1 Å with the crystal structure pose indicating enough docking accuracy. Subsequently, the docking between AzaA and JHE was performed using a similar protocol. The single lowest energy conformation was selected from the largest cluster having binding free energy of −6.94 kcal/mol (Figure 8C). In this conformation, AzaA binds within a long narrow tunnel containing the enzyme active site (Figure 7A). The tunnel opened at the surface of the protein (Figure 7B) that allowed entry and accommodation of AzaA (Figure 7C,D). Hydrophobic residues lining the tunnel interacting with AzaA included Leu-98, Phe-150, Phe-259, Phe-311, Leu-313, Phe-361, Phe-365, Ile-360, and Ile-368 (Figure 6e,f). Moreover, Gly-147, Gly-146, Ala-227, and His-471 underwent direct hydrogen-bonding interactions with AzaA at one end of tunnel (Figure 8A,B). This network of hydrophobic and hydrogen-bonding interactions stabilized AzaA in the substrate binding cavity of JHE. Interestingly, the bound conformation and interaction of AzaA was similar to observed OTFP in the crystal structure. Thus, the theoretical interaction pattern of AzaA with JHE offered a convincing rationale for the results with the labeled compound.

DISCUSSION

The defensive and versatile detoxification mechanism in *H. armigera* is a potential key for their survival. This mechanism may have originally evolved for protection. Another possibility is that it may have been reinforced by the vast use of pesticides used by farmers. Considering this and the desirability of avoiding synthetic pesticides, a multitargeted natural pesticide like AzaA can be of widespread use for insect control. In this context, we have shown how the prolific use of a broad-spectrum AzaA could control insect pests. This biopesticide has the ability to keep the insect engaged in defensive or detoxification interactions while reducing food consumption. Many studies have shown that AzaA is a strong antifeedant.[8,26−31] We confirmed this and additionally demonstrated that the antifeedant action resulted in a less-than-proportional uptake of the compound. This still leaves some scope for intoxication, which would not occur if feeding ceased immediately and completely.

The spatial distribution of AzaA in *H. armigera* within the midgut might be critical in explaining its toxicity in insects. Ion

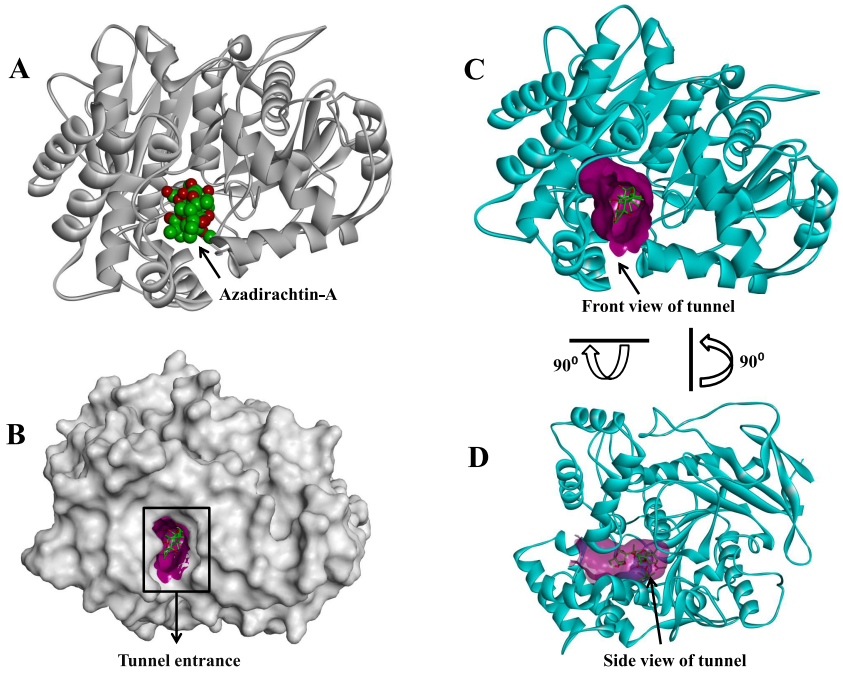

Figure 7. Overall structure of JHE complexed with AzaA and molecular interaction between JHE and AzaA. (A) Cartoon representation of the secondary structure organization of JHE (gray) and bound conformation of AzaA (green) as spacefill representation. (B) Surface representation of JHE (gray) showing location and entrance of tunnel (purple). (C, D) Surface representation showing front and side views of long narrow active site tunnel (purple) with deeply buried AzaA (green stick).

DOI: 10.1021/acsomega.8b03479
ACS Omega 2019, 4, 9531−9541

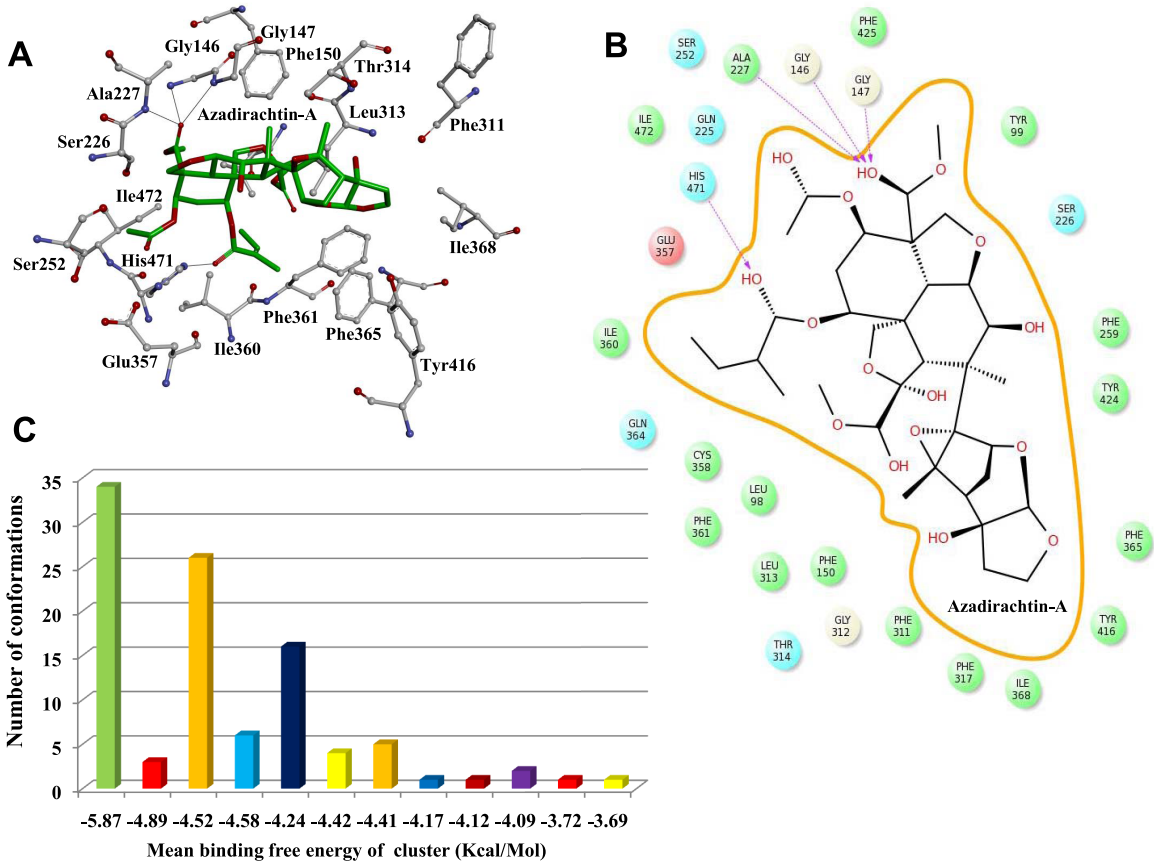

Figure 8. (A) Intramolecular hydrogen bonding (black line) and surrounding hydrophobic residue (gray sticks) of JHE and AzaA (green sticks). (B) Schematic representation showing two-dimensional (2D) interaction plot of AzaA (black wire) with JHE residue. (C) Cluster analysis of docking runs of AzaA binding showing number of conformations vs mean binding energy (kcal/mol).

intensity maps constructed from MALDI-TOF mass spectra demonstrated that some ingested AzaA remained in the midgut of *H. armigera*, where the majority of the digestive, defensive, transport-, detoxification-, and immunity-related mechanisms are controlled. This provides the access for AzaA to interact with multiple targets.

The present metabolomic analysis sheds light on the degradation/catabolism of AzaA by *H. armigera*. The fragmentation pattern and products of AzaA are proposed. General metabolism of *H. armigera* upon AzaA ingestion indicated that many amino acid levels decreased in the larvae. Alteration of primary metabolism was notable even at the lowest (32 ppm) AzaA exposure. All lipids and citrate cycle were strongly affected by AzaA ingestion. Overall data indicated inability of *H. armigera* larvae to metabolize AzaA, and thus the insects could not avoid the toxic effect. Alternately, even metabolized products could also affect primary metabolism of the insect, resulting in antibiosis.

Proteomic examination of AzaA-fed insects revealed regulation of processes that have not been previously reported, such as fatty acid metabolism. Long-distance flight of species like locusts and hawkmoths is fueled through fatty acid oxidation.[32,33] Locust flight muscle cytoplasm contains an abundant fatty acid binding protein (FABP). Recombinant rEs-FABP9 and rEsABP10 are two lipid metabolism-related proteins in the innate immune system of the mitten crab *Eriocheir sinensis* (order, Decapoda; family, Varunidae).[34] As an FABP was downregulated in AzaD-fed *H. armigera*, one effect of AzaA could be to reduce the muscle tone and immunity of the larvae. Cofilin provides another example of a different type of target. Gene ontology indicated that cofilin is mainly involved in the biological process of actin filament depolymerization, i.e., disassembly of actin filaments by the removal of actin monomers. Cofilin regulator 14-3-3 zeta is an evolutionarily conserved protein required for phagocytosis and microbial resistance.[35] In the present study, cofilin was found in reduced level in AzaD-fed *H. armigera*, which could lead to lower immunity of these insects. SODs provide an important cellular enzymatic defense against the detrimental reactive oxygen species generated by aerobic metabolism.[36] GAPDH is known to interact with different biomolecules. Many cellular activities, including programmed cell death and nuclear RNA transport unrelated to the commonly known carbohydrate metabolism, are also affected by GAPDH.[37] Cytochromes P450 are important enzymes and may confer resistance to insecticides.[38] SODs, GAPDH, and P450s were all downregulated in AzaD-fed insects. Protein regulation by AzaA ingestion thereby affected many different biological processes in these insects.

Since AzaA binding may or may not affect the biological activity of a protein, the role of most of these as potential toxic targets of AzaA, identified for the first time here, remains to be investigated. However, we followed up on the binding to JHE by modeling the docking of AzaA. In the highest-affinity conformation, AzaA occupied the active site of JHE, which would be predicted to inhibit its activity toward its natural substrates. Since juvenile hormone affects so many processes in insect differentiation and physiology, perhaps some of the

DOI: 10.1021/acsomega.8b03479
ACS Omega 2019, 4, 9531−9541

effects we have documented result from AzaA binding to the single target JHE. Further research will be required to separate the downstream consequences resulting from the binding of AzaA to various proteins. If several independent targets of AzaA can be demonstrated, this would suggest that it will be more difficult for insects to evolve resistance to AzaA than to many currently used insecticides that have a single major target.

This study confirms the antifeedant and toxic effects of AzaA on the key agricultural pest *H. armigera*, which has evolved resistance to most insecticides in current use. Our observations of a variety of diverse responses at transcript, protein, and metabolite levels, as well as the identification of different binding targets, indicate that the mode of action might exploit many different targets in the insect, making AzaA a promising compound for future development to combat the growing problem of insecticide resistance in this and other crop pests worldwide.

MATERIALS AND METHODS

Chemicals. Acetonitrile, bovine serum albumin, and sequencing grade-modified trypsin were procured from Sigma Chemicals (St. Louis, MO). MassPrep predigested standard protein rabbit glycogen phosphorylase B, RapiGest, and enolase were purchased from Waters Corporation (Manchester, U.K.). All other chemicals of analytical grade were procured locally, in India. Extraction of neem limonoids AzaA from the neem seed kernel was performed as described by Alam et al.[39] 7-Nitrobenzo-2-oxa-1,3-diazole (NBD)-based labeled AzaA was used for gel electrophoresis experiments.[40]

Insect Feeding and Collection of Tissues. Actively feeding *H. armigera* larvae collected from fields were transferred and maintained on artificial diet (AD).[41] Azadirachtin-A-based diet (AzaD) was prepared in four concentrations by adding AzaA (0, 32, 64, and 128 ppm in 70% ethanol) to AD. To ensure greater genetic homogeneity among test populations, the insects were maintained on AD for three generations. To understand the effect of AzaD on growth and development of *H. armigera*, a set of insects were fed on AD up to early fourth instar and then transferred to AzaD. After transfer to AzaD, the insects were fed about 96 h continuously on it and used for collecting the insect tissue samples. For control group, the insects were continuously grew on AD and harvested at the same time. Furthermore, to observe insect performance on AzaD, the insects were fed on the AD and AzaD continuously and larvae were carefully weighed after every 24 h. For metabolomics analysis, the insects were anesthetized by chloroform and snap-frozen in liquid nitrogen. Larvae were stored at −20 °C until further analysis. For MALDI imaging, *H. armigera* larvae were grown on an artificial pinto bean-based diet (AD) till early fourth instar stage. AzaD was prepared by mixing AzaA (64 ppm) in artificial pinto bean-based diet. Samples for MALDI imaging were collected from insects shifted from AD to AzaD as described above.

MALDI Imaging. Insects which fed on AD and AzaD were anesthetized by chloroform and snap-frozen in liquid nitrogen. Larvae were manually cut into three pieces by using a blade, in an attempt to isolate foregut, midgut, and hindgut. Cryosections (16 μm) of insects were taken by using a Leica cryomicrotome (Leica CM1850, Leica Mikrosysteme Vertrieb, Germany). The cross sections were attached by thawing on a MALDI stainless steel target plate (Waters) and quickly transferred into a desiccator for drying. The target plate was kept in a vacuum desiccator, dried for 3−4 h, and then sublimated with 2,5-dihydroxybenzoic acid (DHB) at 140 °C for 5 min at 0.05 Torr. A MALDI microMX mass spectrometer (Waters) fitted with a nitrogen laser (337 nm, 4 ns laser pulse duration, 10 Hz, and 154 μJ per pulse) was used in reflectron mode and positive polarity for data acquisition using MassLynx version 4.0 software. The *x*, *y* coordinates for the imaging acquisition were defined by using proprietary software with 50 μm step size. Data collected with MassLynx 4.0 were processed with custom-made software MALDI Image Converter (Waters). Finally, the data were exported to ImageJ (National Institute of Health, Bethesda, MD) and converted into two-dimensional ion intensity maps. The converted data files were imported into Biomap (Novartis, Basel, Switzerland) for image visualization and processing. The chemical identity of the compounds was confirmed by mass spectrometry on an LTQ Orbitrap XL mass spectrometer (Thermo Fisher Scientific, Bremen, Germany) with an ESI source and Excalibur v.2.0 (Thermo Fisher Scientific, Waltham, MA) software for data acquisition.

Metabolomics Analysis. Four AzaD-fed larval groups (0, 32, 64, and 128 ppm AzaD-fed larvae) were analyzed for metabolomics. In brief, three frozen larvae from a single AzaD-fed group were pooled up together as one biological replicate. Three such replicates were performed for each AzaD-fed group. Each replicate was weighed and ground into a powder in liquid nitrogen using a mortar and pestle. Around 150−200 mg of powder (visibly 1/10 of the vial of 4.5 mL capacity) was transferred into a liquid nitrogen precooled glass vial (4.5 mL capacity). Extraction solvent mixture was added according to the weight of tissue (2 mL extraction solvent/100 mg tissue) in the vials. The extraction solvent consisted of MeOH (50 mL), ethyl acetate (50 mL), $^{13}C_6$-glucose (1 mL, 10 mg/mL), $^{13}C_6$-phenylalanine (100 μL, 10 mg/mL), and D_{27}-palmitic acid (1 mL, 10 mg/mL) solutions made in MeOH/ethyl acetate mixture. Each vial was vortexed for 3−5 s and then sonicated for 15 min at room temperature (24 °C). During sonication, the vials were once inverted and mixed at the seventh minute. The vials were centrifuged at 2000*g* for 10 min at 4 °C and the supernatant was separated from debris, stored in glass vials (4.5 mL), and kept at −80 °C prior analysis.

Ultra-high-performance liquid chromatography-electrospray ionization mass spectrometry (UHPLC−ESI−MS) was performed with the larval extract using the Ultimate 3000 series RSLC (Dionex, Sunnyvale, CA) system coupled to a Q-Exactive Plus hybrid quadrupole-orbitrap (Q-Exactive Plus) mass spectrometer (Thermo Fisher Scientific GmbH, Bremen, Germany) equipped with an ESI source. A 2 μL volume of the extract was injected into the UHPLC binary solvent system of water (solvent A) and acetonitrile (solvent B, hyper grade for LC−MS, Merck, Darmstadt, Germany), both containing 0.1% (v/v) formic acid (eluent additive for LC−MS, Sigma-Aldrich, Steinheim, Germany). Chromatographic separation was achieved using an Acclaim C18 column (150 × 2.1 mm^2, 2.2 μm; Dionex, Sunnyvale, CA) at a constant flow rate of 300 μL/min as follows: 0.0−100% (v/v) B (in 15 min) and held at 100% B for 10 min. A mass spectrometer was set for positive- or negative-ion mode acquisition with an ESI voltage to 35 V, mass resolution to 70 000 full width at half-maximum (FWHM), and mass acquisition range to m/z 100−1500. Tandem mass spectra for the extracts were obtained on the same instrumental setup with the following parameters: survey

DOI: 10.1021/acsomega.8b03479
ACS Omega 2019, 4, 9531−9541

scan at 70 000 FWHM was followed by TOPN ddMS/MS scan with quadrupole selection window 0.8 Da, ion count threshold of 5.3e4, automatic gain control target 1e6, and maximum IT time of 150 ms with 35 000 FWHM mass resolutions. Higher-energy collisional dissociation (HCD) fragmentations were performed in a quadrupole with nitrogen as collision gas with ramped normalized collision energy in steps 10, 30, 60 V. Dynamic exclusion window was set to 2700 s.

A total of 20 pure metabolite standards (including AzaA) were measured in LC−MS under similar condition to obtain the reference retention times. Structural elucidation for metabolites not included in the standards were performed from TOPN-derived HCD spectra using accurate mass and isotopic pattern for full MS data and from comparing HCD data with our internal and public (MassBank, METLIN) databases. Data analysis was accomplished using Excalibur v.3.0.63 (Thermo Fisher Scientific, Waltham, MA). Relative quantification of identified metabolites was performed by relating the total ion intensity of metabolite peak to the total ion intensity of one of the three labeled internal standards added to extracts (Suppl. Data 2−4).

The first aspect of metabolomics analysis was to investigate the potential transformation products and/or metabolites of AzaA (Suppl. Figure 1) in *H. armigera*. It was divided in two approaches: (i) to elucidate the MS fragmentation pathway of AzaA and (ii) to study the expected degradation or biotransformation within the chemical structure of AzaA, according to the most common biotransformation pathways for detoxification in insect metabolism, to establish a direct relationship between the precursor AzaA and its metabolites.

The second aspect of metabolomics analysis was to elucidate the effect of AzaA on the general metabolism of *H. armigera*. In this aspect, we initially made a list of metabolites of interest coming from various metabolite classes such as amino acids, fatty acids, sugars, and glycolysis/citrate pathway intermediate (Suppl. Table 1). In the list, 32 metabolites could be detected reliably in LC−MS on the basis of their reproducible retention time and peak shape. Thus, we showed data for these 32 metabolites only (Suppl. Table 2). Among the 32 metabolites, retention times for 20 metabolites were obtained using standards. These 20 metabolites were identified in larval extracts on the basis of retention time and exact monoisotopic mass (such metabolite's names are suffixed as "_true" in the supplementary XLS file; Suppl. Data 1). Other metabolites were putatively identified on the basis of exact monoisotopic mass (±5 ppm). LC−MS data were acquired in both positive- and negative-ion modes. LC−MS peak areas were calculated for the metabolite ions $[M + H]^+$, $[M + Na]^+$, and $[M - H]^-$ separately (Suppl. Data 2−4) using ThermoXcalibur processing setup-Quan identification browser (Thermo Fisher Scientific, Waltham, MA) and averaged for three replicates, plotted over AzaD concentrations (Suppl. Data 1). Finally, we normalized the lowest LC−MS peak area to 1 among the four AzaA feeding groups to simplify outlook and visualize the up/downregulation trend of a particular metabolite by relative peak area comparison (Suppl. Data 1).

Proteomic Analysis. Proteins from gut were extracted by the phenol method according to the Schuster and Davies[42] protocol with slight modifications. Proteins from *H. armigera* hemolymph were extracted by a trichloroacetic acid−acetone method.[43] Target identification with the help of the proteomic approach by using 7-nitrobenzo-2-oxa-1,3-diazole (NBD)-based labeled AzaA was carried out with the in-gel digestion protocol.[41]

Proteins were extracted from AD-fed whole larvae and mixed with labeled AzaA and incubated in the dark at 24 °C for 2 h. This incubated protein mixture (20 μg each) was loaded onto a 15% polyacrylamide separation gel with a 4% stacking gel and electrophoresed at 20 °C using a vertical polyacrylamide gel electrophoresis apparatus.[44] The gels were run at a constant current of 50 A/gel until the fluorescent band reached the bottom of the gel. The electrophoresis was carried out in the dark to avoid quenching of fluorescently labeled AzaA. The gels were visualized by using a transilluminator (Bio-Rad UV Transilluminator 2000, Hercules, CA). Fluorescent protein bands were excised from the PAGE gels, in-gel digestion, and a NanoAcquity ultraperformance liquid chromatography (UPLC) coupled to MALDI-SYNAPT-HDMS (Waters) was performed for proteomic analysis, as reported by Dawkar et al.[41]

Data processing and database searching and the continuum LC−MS^E data were processed and analyzed using Protein Lynx Global Server 2.5.2 software (PLGS, Waters), and protein identifications were done by the Lepidopteran database (www.uniprot.org). Data-independent MS^E data sets for the ion accounting search algorithm within PLGS were investigated according to Li et al.[45] Digested enolase (100 fmol) was spiked in the samples to quantify the protein samples. Three biological replicates (30 insects in each) were used for all experiments.

Molecular Docking Study of AzaA with *H. armigera* Juvenile Hormone Esterase. The structure of AzaA (CID 5281303) was obtained from the PubChem compounds database. The geometry optimization and partial atomic charges were assigned to ligand molecule using Gaussian 09 program.[46] The X-ray structure of juvenile hormone esterase (JHE) covalently bound with inhibitor 3-octylthio-1,1,1-trifluoropropan-2-one (OTFP) (PDB ID: 2FJ0) was retrieved from Protein Data Bank.[47] The ligand was extracted from PDB file and hydrogen atom was added. The Kollman united atom charges and protonation state were assigned to receptor atom.[24] Molecular docking has been performed between JHE and AzaA using AutoDock 4.2.[24] The residues known to play important roles in JHE activity and substrate binding (Gly-146, Ser-226, Ala-227, Phe-259, Leu-313, Thr-314, Glu-357, Phe-361, Tyr-424, and His-471) were treated as flexible.[47] The grid box was set to 70 × 60 × 56 points with a grid spacing of 0.375 Å centered on the selected flexible residue and active site of JHE. The grid box contains the entire binding site of JHE, which provides enough space for translation (0.25 Å) and rotation (5°) of the ligand, with the rest of the docking parameters kept to their default values. Thus, 100 docking rounds were performed. The generated docked conformations were clustered with an RMSD tolerance of 1.5 Å and ranked by predicted binding free energy.

Gene Expression Analysis by Quantitative Real-Time PCR (qPCR). To evaluate the expression pattern of genes on AzaD, relative transcript levels of selected target genes were checked for respective treatment diets. Overall, 15 genes were considered from the proteomics data. Total RNA for one biological replicate was isolated from pools of 10 larvae using Trizol reagent (Invitrogen, Carlsbad, CA). Synthesis of cDNA was done by High Capacity cDNA Reverse Transcription Kit (Applied Biosystems). qPCR was performed using the 7900HT Fast Real-Time PCR System (Applied Biosystems)

DOI: 10.1021/acsomega.8b03479
ACS Omega 2019, 4, 9531−9541

to examine transcript abundance of selected target mRNAs. RT-qPCR analyses were done as described earlier.[48] The list of primers used for RT-qPCR analyses is given in Suppl. Table 3.

Statistical Analysis. Data were analyzed by one-way analysis of variance with Tukey−Kramer multiple comparisons tests. All of the data were expressed as mean ± standard error. Data points were considered significant at $p \leq 0.05$, $p \leq 0.01$, and $p \leq 0.0001$.

■ ASSOCIATED CONTENT

Supporting Information

The Supporting Information is available free of charge on the ACS Publications website at DOI: 10.1021/acsomega.8b03479.

Chemical structure of azadirachtin-A; chromatographic traces of azadirachtin-A from extract of *H. armigera*; MS/MS spectra of azadirachtin-A adduct ions; representation of the azadirachtin-A response in LC−MS; list of metabolites; common biotransformation metabolites proposed for azadirachtin-A degradation pathway; list of primers (PDF)

List of identified proteins (XLSX)(XLSX)

Up- or downregulation trend of a particular metabolite by relative peak area comparison; cumulative list of all positively and negatively identified metabolites; and peak area and relative quantification of metabolites (XLSX)(XLSX)(XLSX)(XLSX)

■ AUTHOR INFORMATION

Corresponding Author

*E-mail: vv.dawkar@ncl.res.in. Tel: +91 (0)20 25902710. Fax: +91 (0)20 25902648.

ORCID

Vishal V. Dawkar: 0000-0003-4135-692X

Notes

The authors declare no competing financial interest.

■ ACKNOWLEDGMENTS

V.V.D. acknowledges the Science and Engineering Research Board, Department of Science and Technology, Govt. of India, New Delhi, for funding under Young Scientist Scheme (SB/YS/LS-260/2013); the Max Planck Institute for Chemical Ecology, Jena, Germany, for awarding a Postdoctoral Research Fellowship; and the Max-Planck-Gesellschaft for financial support of the research.

■ REFERENCES

(1) Kraus, W. In *The Neem Tree: Source of Unique Natural Products for Integrated Pest Management, Medicine, Industry and Purposes*; Schmutterer, H., Ed.; VCH Weinheim: Germany, 1995; Vol. *696*, pp 35−88.

(2) Singh, R. P.; Chari, M. S.; Raheja, A. K.; Kraus, W. *Neem and Environment*; Oxford & IBH Publishing: New Delhi, 1996; Vols. *I−II*, pp 1−1198.

(3) Ascher, K. R. S. Nonconventional insecticidal effects of pesticides available from neem tree, *Azadirachta indica*. *Arch. Insect Biochem. Physiol.* **1993**, *22*, 433−449.

(4) Butterworth, J. H.; Morgan, E. D. Isolation of a substance that suppresses feeding in locusts. *Chem. Commun.* **1968**, *4*, 23−24.

(5) Zebitz, C. P. W. Effect of some crude and azadirachtin-enriched neem (*Azadirachta indica*) seed kernel extracts on larvae of *Aedes aegypti*. *Entomol. Exp. Appl.* **1984**, *35*, 11−16.

(6) Huang, Z.; Shi, P.; Dai, J.; Du, J. Protein metabolism in *Spodoptera litura* (F.) is influenced by the botanical insecticide azadirachtin. *Pestic. Biochem. Physiol.* **2004**, *80*, 85−93.

(7) Jacobson, M. *The Neem Tree: Natural Resistance Par Excellence*; ACS Symposium Series; American Chemical Society: Washington, DC, 1986; Vol. *296*, pp 220−232.

(8) Rembold, H. In *Focus on Phytochemical Pesticides, The Neem Tree*; Jacobson, M., Ed.; CRC Press: Boca Raton, 1989; Vol. *1*, pp 47−67.

(9) Khalil, M. S. Abamectin and azadirachtin as eco-friendly promising biorational tools in integrated nematodes management programs. *J. Plant Pathol. Microbiol.* **2013**, *4*, 174.

(10) Nisbet, A. J.; Mordue, A. J.; Mordue, W.; Williams, L. M.; Hannah, L. Autoradiographic localisation of [22,23-3H2] dihydroazadirachtin binding sites in desert locusts testes. *Tissue Cell* **1996**, *28*, 725−729.

(11) Roy, S.; Gurusubramanian, G. Bioefficacy of azadirachtin content of neem formulation against three major sucking pests of tea in Sub Himalayan tea plantation of North Bengal, India. *Agric. Trop. Subtrop.* **2011**, *44*, 134−143.

(12) Shi, P.; Huang, Z.; Chen, G.; Zhou, L.; Tan, X. Effects of azadirachtin on six inorganic cation distributions in *Ostrinia furnacalis* (G.). *Biol. Trace Elem. Res.* **2006**, *113*, 105−112.

(13) Wang, H.; Lai, D.; Yuan, M.; Xu, H. Growth inhibition and differences in protein profiles in azadirachtin-treated *Drosophila melanogaster* larvae. *Electrophoresis* **2014**, *35*, 1122−1129.

(14) Ley, S. V.; Denholm, A. A.; Wood, A. The chemistry of azadirachtin. *Nat. Prod. Rep.* **1993**, *10*, 109−157.

(15) Mordue, A. J.; Simmonds, M. S. J.; Ley, S. V.; Blaney, W. M.; Mordue, W.; Nasiruddin, M.; Nisbet, A. J. Actions of azadirachtin, a plant allelochemical, against insects. *Pest Manage. Sci.* **1998**, *54*, 277−284.

(16) Mordue, A. J.; Blackwell, A. Azadirachtin - an Update. *J. Insect Physiol.* **1993**, *39*, 903−924.

(17) Hassanali, A.; Bentley, M. D. In *Comparison of the Insect Antifeedant Activities of Some Limonoids*, Proceedings of the 3rd International Neem Conference, Nairobi, Kenya, 10−15 July, 1986; pp 683−689.

(18) Sharma, H. C. *Crop Protection Compendium*; Common Wealth Agricultural Bureau International: Wallingford, U.K., 2001.

(19) www.pesticideresistance.org/.

(20) www.iraconline.org/.

(21) Bauer, L. S. Resistance: A threat to the insecticidal crystal proteins of *Bacillus thuringiensis*. *Fla. Entomol.* **1995**, *78*, 414−443.

(22) Dawkar, V. V.; Chikate, Y. R.; Lomate, P. R.; et al. Molecular insights in to detoxification mechanisms of Lepidopteron insect pests. *J. Proteome Res.* **2013**, *12*, 4727−4737.

(23) Tabashnik, B. E. Evolution of resistance to *Bacillus thuringiensis*. *Ann. Rev. Entomol.* **1994**, *39*, 47−79.

(24) Morris, G. M.; Huey, R.; Lindstrom, W.; Sanner, M. F.; Belew, R. K.; Goodsell, D. S.; Olson, A. J. AutoDock4 and AutoDockTools4: Automated docking with selective receptor flexibility. *J. Comput. Chem.* **2009**, *30*, 2785−2791.

(25) Wogulis, M.; Wheelock, C. E.; Kamita, S. G.; et al. Structural studies of a potent insect maturation inhibitor bound to the juvenile hormone esterase of *Manduca sexta*. *Biochemistry* **2006**, *45*, 4045−4057.

(26) Gopalakrishnan, G.; Singh, N. D. P.; Kasinath, V.; Krishnan, M. S. R.; Malathi, R.; Rajan, S. S. Microwave- and ultrasound-assisted oxidation of bio-active limonoids. *Tetrahedron Lett.* **2001**, *42*, 6577.

(27) Hossain, M. M.; Sultana, F.; Kubota, M.; Hyakumachi, M. Differential inducible defense mechanisms against bacterial speck pathogen in *Arabidopsis thaliana* by plant-growth-promoting-fungus *Penicillium* sp. GP16-2 and its cell free filtrate. *Plant Soil* **2008**, *304*, 227.

(28) Ley, S. V. Synthesis of antifeedants for insects: novel behaviour-modifying chemicals from plants. *Ciba Found. Symp.* **1990**, *154*, 80−87 discussion 87−98. .

DOI: 10.1021/acsomega.8b03479
ACS Omega 2019, 4, 9531−9541

(29) Madyastha, K. M.; Venkatakrishnan, K. Biocatalyst-mediated expansion of ring D in azadirachtin, a potent insect antifeedant from *Azadirachta indica*. *Tetrahedron Lett.* **1999**, *40*, 5243−5246.
(30) Mordue (Luntz), A. J.; Nisbet, A. J.; Nasiruddin, M.; Walker, E. Differential thresholds of azadirachtin for feeding deterrence and toxicity in locusts and an aphid. *Entomol. Exp. Appl.* **1996**, *80*, 69−72.
(31) Simmonds, M. S.; Jarvis, A. P.; Johnson, S.; Jones, G. R.; Morgan, E. D. Comparison of anti-feedant and insecticidal activity of nimbin and salannin photo-oxidation products with neem (*Azadirachta indica*) limonoids. *Pest Manage. Sci.* **2004**, *60*, 459−464.
(32) Goh, K. S.; Li, C. W. A photocytes-associated fatty acid-binding protein from the light organ of adult Taiwanese firefly, *Luciola cerata*. *PLoS One* **2011**, *6*, No. e29576.
(33) van der Horst, D. J.; van Doorn, J. M.; Passier, P. C.; Vork, M. M.; Glatz, J. F. Role of fatty acid-binding protein in lipid metabolism of insect flight muscle. *Mol. Cell. Biochem.* **1993**, *123*, 145−152.
(34) Cheng, L.; Jin, X. K.; Li, W. W.; Li, S.; Guo, X. N.; Wang, J.; Gong, Y. N.; He, L.; Wang, Q. Fatty acid binding proteins FABP9 and FABP10 participate in antibacterial responses in Chinese mitten crab, *Eriocheir sinensis*. *PLoS One* **2013**, *8*, No. e54053.
(35) Ulvila, J.; Vanha-aho, L. M.; Kleino, A.; Vaha-Makila, M.; Vuoksio, M.; Eskelinen, S.; Hultmark, D.; Kocks, C.; Hallman, M.; Parikka, M.; Ramet, M. Cofilin regulator 14-3-3zeta is an evolutionarily conserved protein required for phagocytosis and microbial resistance. *J. Leukocyte Biol.* **2011**, *89*, 649−659.
(36) Fridovich, I. Superoxide radical and superoxide dismutases. *Annu. Rev. Biochem.* **1995**, *64*, 97−112.
(37) Chong, I. K.; Ho, W. S. Glyceraldehyde-3-phosphate dehydrogenase from Chironomidae showed differential activity towards metals. *Protein Pept. Lett.* **2013**, *20*, 970−976.
(38) Scott, J. G.; Wen, Z. M. Cytochromes P450 of insects: the tip of the iceberg. *Pest Manage. Sci.* **2001**, *57*, 958−967.
(39) Alam, A.; Haldar, S.; Thulasiram, H. V.; et al. Novel anti-inflammatory activity of epoxyazadiradione against macrophage migration inhibitory factor: inhibition of tautomerase and proinflammatory activities of macrophage migration inhibitory factor. *J. Biol. Chem.* **2012**, *287*, 24844−24861.
(40) Haldar, S.; Kumar, S.; Kolet, S. P.; Patil, H. S.; Kumar, D.; Kundu, G. C.; Thulasiram, H. V. One-pot fluorescent labeling protocol for complex hydroxylated bioactive natural products. *J. Org. Chem.* **2013**, *78*, 10192−10202.
(41) Dawkar, V. V.; Chikate, Y. R.; Gupta, V. S.; Slade, S. E.; Giri, A. P. Assimilatory potential of *Helicoverpa armigera* reared on host (Chickpea) and nonhost (*Cassia tora*) diets. *J. Proteome Res.* **2011**, *10*, 5128−5138.
(42) Schuster, A.; Davies, E. Ribonucleic acid and protein metabolism in *Pea Epicotyls*: III. Response to auxin in aged tissue. *Plant Physiol.* **1983**, *73*, 822−827.
(43) Méchin, V.; Damerval, C.; Zivy, M. Total Protein Extraction with TCA-Acetone. In *Plant Proteomics*; Thiellement, H. et al., Ed.; Methods in Molecular Biology; Humana Press, 2007; Vol. 355, pp 1−8.
(44) Bradford, M. M. A rapid and sensitive method for the quantitation of microgram quantities of protein utilizing the principle of protein-dye binding. *Anal. Biochem.* **1976**, *72*, 248−254.
(45) Li, G. Z.; Vissers, J. P.; Silva, J. C.; Golick, D.; Gorenstein, M. V.; Geromanos, S. J. Database searching and accounting of multiplexed precursor and product ion spectra from the data independent analysis of simple and complex peptide mixtures. *Proteomics* **2009**, *9*, 1696−1719.
(46) Frisch, M. J.; Trucks, G. W.; Schlegel, H. B.; Scuseria, G. E.; Robb, M. A.; Cheeseman, J. R.; Scalmani, G.; Barone, V.; Mennucci, B.; Petersson, G. A.; Nakatsuji, H.; Caricato, M.; Li, X.; Hratchian, H. P.; Izmaylov, A. F.; Bloino, J.; Zheng, G.; Sonnenberg, J. L.; Hada, M.; Ehara, M.; Toyota, K.; Fukuda, R.; Hasegawa, J.; Ishida, M.; Nakajima, T.; Honda, Y.; Kitao, O.; Nakai, H.; Vreven, T.; Montgomery, J. A., Jr.; Peralta, J. E.; Ogliaro, F.; Bearpark, M.; Heyd, J. J.; Brothers, E.; Kudin, K. N.; Staroverov, V. N.; Kobayashi, R.; Normand, J.; Raghavachari, K.; Rendell, A.; Burant, J. C.; Iyengar, S. S.; Tomasi, J.; Cossi, M.; Rega, N.; Millam, J. M.; Klene, M.; Knox, J. E.; Cross, J. B.; Bakken, V.; Adamo, C.; Jaramillo, J.; Gomperts, R.; Stratmann, R. E.; Yazyev, O.; Austin, A. J.; Cammi, R.; Pomelli, C.; Ochterski, J. W.; Martin, R. L.; Morokuma, K.; Zakrzewski, V. G.; Voth, G. A.; Salvador, P.; Dannenberg, J. J.; Dapprich, S.; Daniels, A. D.; Farkas, Ö.; Foresman, J. B.; Ortiz, J. V.; Cioslowski, J.; Fox, D. J. *Gaussian 09*, revision A; Gaussian, Inc.: Wallingford, CT, 2009.
(47) Wogulis, M.; Wheelock, C. E.; Kamita, S. G.; Hinton, A. C.; Whetstone, P. A.; Hammock, B. D.; Wilson, D. K. Structural studies of a potent insect maturation inhibitor bound to the juvenile hormone esterase of *Manduca sexta*. *Biochemistry* **2006**, *45*, 4045−4057.
(48) Chikate, Y. R.; Tamhane, V. A.; Joshi, R. S.; Gupta, V. S.; Giri, A. P. Differential protease activity augments polyphagy in *Helicoverpa armigera*. *Insect Mol. Biol.* **2013**, *22*, 258−272.

DOI: 10.1021/acsomega.8b03479
ACS Omega 2019, 4, 9531−9541